Bergische Universität Wuppertal

Fachbereich Mathematik und Naturwissenschaften

Lehrstuhl für Angewandte Mathematik
und Numerische Mathematik

Lehrstuhl für Optimierung und Approximation

Matthias Ehrhardt

# An Introduction to Fluid-Porous Interface Coupling

October 2010

http://www.math.uni-wuppertal.de

# An Introduction to Fluid-Porous Interface Coupling

## M. Ehrhardt

*Bergische Universität Wuppertal, Fachbereich Mathematik und Naturwissenschaften, Lehrstuhl für Angewandte Mathematik und Numerische Mathematik, Gaußstrasse 20, 42119 Wuppertal, Germany.*

Abstract: Numerical simulation of coupled flows in plain and porous media is essential for many industrial and environmental problems. In this introductory chapter we shortly review coupling conditions between the pure liquid flow and the flow in a porous medium. Hereby, we will discuss the two well studied cases of normal and parallel flow over a porous layer ans focus on the later one.

As an application, we present two examples modelling Proton exchange membrane (PEM) fuel cells and an electrochemical channel flow cell.

After discussing different mathematical models this chapter will focus on the description of the coupling of the free flow in the channel region with the filtration velocity in the porous diffusion layer as well as interface conditions between them.

The difficulty in finding effective coupling conditions at the interface between the channel flow and the porous layer lies in the fact that often the orders of the corresponding differential operators are different, e.g. when using (Navier-) Stokes and Darcy's equation. Alternatively, using the Brinkman model for the porous media this difficuly does not occur. We will review different interface conditions, including the well-known Beavers-Joseph-Saffman boundary condition and its recent improvement by Le Bars and Worster.

Finally, three different mathematical models for fluid–porous interfaces in a simple channel geometry are discussed and explicit Poiseuille-like solutions for the flow velocity are derived that can lead to semi-analytic numerical methods.

## 1. INTRODUCTION

Numerical simulation of coupled flows in plain and porous media is essential for many industrial and environmental problems, like *proton exchange membrane (PEM) fuel cells*, flow through oil filters [19], contaminant transport from lakes by groundwater, flow in bioreactors, contaminant gas leaking from atomic waste containers in deep rock depositories, $CO_2$ sequestration in the subsurface, salt water intrusion (sensitive density driven flow), cancer therapy, etc..

In this work we will focus on coupling conditions between the pure liquid flow and the flow in the porous media. Hereby, we will discuss the two well studied cases of normal and parallel flow over a porous layer ans focus on the later one Furthermore, we regard mass transport from the fluid region to the porous layer.

As an application, we present two examples modelling Proton exchange membrane (PEM) fuel cells and an electrochemical channel flow cell.

**Example 1.1** (PEM Fuel Cell). *In Proton exchange membrane (PEM) fuel cells, the transport of the fuel to the active zones, and the removal of the reaction products are realized using a combination of channels and porous diffusion layers. In order to improve existing mathematical and numerical models of PEM fuel cells, a deeper understanding of the coupling of the flow processes in the channels and diffusion layers is necessary.*

*In general, we distinguish two types of PEM fuel cells: $H_2$ PEM fuel cells ($H_2$PEMFC) driven by gaseous hydrogen, and direct methanol fuel cells (DMFC) operating on methanol in an aqueous solution. Both anode and cathode consist of supply channels, a porous diffusion layer and an active zone. They are connected by a proton conducting membrane. For details we refer the interested reader to [13], [14].*

*The most important chemical reactions in PEM fuel cells are at the anode*

**DMFC** $CH_3OH + H_2O \rightarrow CO_2 + 6H^+ + 6e^-$

**PEMFC** $3H_2 \rightarrow 6H^+ + 6e^-$
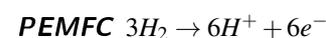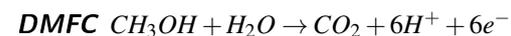
*and at the cathode $\frac{3}{2}O_2 + 6H^+ + 6e^- \rightarrow 3H_2O$.*
*Consequently, in an $H_2$PEMFC, ideally, the anode contains only hydrogen, while the cathode contains a mixture of liquid water, water vapour and oxygen*

*resp. air. While for an optimal supply of oxygen, it is desirable to keep the amount of liquid water at the cathode minimal, the optimal proton conductivity of the membrane is reached only if it contains enough water. Hence, the water management is an essential issue.*

*In a DMFC, which is operated on an aqueous solution of methanol, we always can assume that the membrane is wet enough to ensure high conductivity. However for this type of fuel cell, methanol permeation through the membrane, leading to a parasitic reaction on the cathode side, is a key problem. Another problem is clogging of the anodic channels by $CO_2$ bubbles.*

*In spite of our remark on the validation of current coupling models, most models either focus on the processes in the membrane electrode assembly (MEA), or in the fluidic channels, simplifying the other process, respectively. A further complication comes from the fact that in both cases, the general process includes two phase flow of a fluid and a gas mixture.*

**Example 1.2** (Flow Cell). *Secondly, we investigate in Section 5 a hypothetical electrochemical channel flow cell which includes a porous diffusion layer covering the anode. Such a structure is close to a fuel cell electrode which usually includes a porous diffusion layer, and therefore the investigation of the influence of the interface between free and porous media flow on solute transport processes appears to be of considerable interest. For the proposed structure, we can use Poiseuille like solutions to obtain coupled free and porous media flow velocity fields.*

The difficulty in finding effective coupling conditions at the interface between the channel flow and the porous layer lies in the fact that, when using stationary (Navier–)Stokes and Darcy's equations to model flow in the two regions, the structures of the corresponding differential operators are different. Alternatively, when using the Brinkman model for the porous media, this difficulty does not occur: continuity of velocity and stress at the interface can be satisfied. But the validity of the Brinkman model for general porous media is discussed controversially, see [33].

We focus on three models: first on the coupling of the free flow with a Darcy medium, secondly the coupling with a Brinkman porous medium and finally we consider a three-layer configuration, where the porous medium is modeled by a Brinkman porous transition layer overlying a Darcy porous material. Exact analytical solutions can be devised

from appropriate interface conditions [6, 17, 35]. The evolution of the species concentration transported with the coupled free and porous media flow is modeled by a standard advection diffusion ansatz. Also, in simple geometries, analytical solutions do not exist, and for a significant range of flow rates of interest, asymptotic theory is not applicable even in the case without a porous layer, calling for numerical methods to obtain approximate solutions for the species concentration.

All numerical algorithms for solving the coupled system of free fluid and porous media can be traditionally classified into two groups of methods.

The first group of methods uses *different equations in different subdomains*, e.g., the Navier–Stokes equation in the liquid region and the Darcy / Brinkman model in the porous zones and couples them through suitable interface conditions. These kind of algorithms are (naturally) based on *domain decomposition* techniques [9]. The advantage of this approach is that one can use existing algorithms and software for solving Navier–Stokes equations and porous media flows. However, the problem of this two–domain approach lies in coupling the conservation equations in both regions through the use of appropriate boundary conditions at the interface.

The second group consists of those algorithms, that solely uses *one system of equations in the whole domain* (Navier–Stokes–Brinkman system) obtaining the transition between both fluid and porous regions through continuous spatial variations of properties ('single-domain approach'). Usually, like in most commercial CFD software (e.g. Star-CD, FLUENT, etc.), the Navier–Stokes–Brinkman system is solved by algorithms developed for the Navier–Stokes system modified such that the main term describing the flow through the porous media is treated explicitly.

## 2. MATHEMATICAL MODELS

In this section we will review some adequate (macroscopic) stationary mathematical models for the flow in each subdomain. In the following $\Omega_f$ denotes the pure fluid domain and $\Omega_p$ is the porous region (membrane). It is essential to recognize that the velocity and pressure variables in $\Omega_f$ and $\Omega_p$ have different meanings but we will use the same notation for both. While in the fluid part **u** and $p$ denote the usual velocity and pressure, in the porous media **u** and $p$ are spatially averaged (over a *representative elementary volume* (REV)) microscopic quantities. The velocity in the porous domain $\Omega_p$ is often referred to volumetric flux density, *Darcy velocity* or *filtration velocity*.

## 2.1 Models in the Free Fluid Region

The free flow in the fluid region $\Omega_f$ is usually modelled by the laminar *incompressible isothermal Navier–Stokes equations* (or by Stokes equations, i.e. neglecting the convective term $(\rho\mathbf{u}\cdot\nabla)\mathbf{u}$ in the case of creeping flows):

$$-\mu\Delta\mathbf{u}+(\rho\mathbf{u}\cdot\nabla)\mathbf{u}=\mathbf{f}_{\mathrm{NS}}-\nabla p \quad (x,y)\in\Omega_f,$$
$$\nabla\cdot\mathbf{u}=g_{\mathrm{NS}} \quad \text{in } \Omega_f, \qquad (1)$$

where $g_{\mathrm{NS}}$ denotes an external source or sink and

$$\Delta\mathbf{u}=[\Delta u^1,\ldots,\Delta u^N]^\top,$$
$$(\mathbf{u}\cdot\nabla)\mathbf{u}=\left[\mathbf{u}\cdot\nabla u^1,\ldots,\mathbf{u}\cdot\nabla u^N\right]^\top,$$

with the velocity vector

$$\mathbf{u}=(u^1,\ldots,u^N)^\top,$$

for dimensions $N=2,3$. In (1) $p$ is the pressure, $\mu$ the fluid viscosity and $\rho$ denotes the density.

## 2.2 Macroscopic Models in the Porous Media

Usually the saturated flow in the porous media $\Omega_p$ is described by the famous *Darcy model* discovered empirically in 1856

$$\mu\mathbf{K}^{-1}\mathbf{u}=\mathbf{f}_{\mathrm{D}}-\nabla p \quad \text{in } \Omega_p,$$
$$\nabla\cdot\mathbf{u}=0 \quad \text{in } \Omega_p, \qquad (2)$$

with $\mu$ the fluid dynamic viscosity, $\mathbf{K}$ permeability tensor of the porous medium and $\mathbf{f}_{\mathrm{D}}$ is a force term (e.g. the gravity). In eq. (2) $\mathbf{u}$ denotes the volumetric average of the velocity and $p$ is the average of the pressure.

An extension of this model (2), the *Brinkman model* [4], is usually used in order to account for the *high porosity* of the porous media or to impose no–slip conditions on solid walls:

$$-\nabla\cdot(\mu_{\mathrm{eff}}\nabla\mathbf{u})+\mu\mathbf{K}^{-1}\mathbf{u}=\mathbf{f}_{\mathrm{B}}-\nabla p \quad \text{in } \Omega_p,$$
$$\nabla\cdot\mathbf{u}=0 \quad \text{in } \Omega_p, \qquad (3)$$

where $\mu_{\mathrm{eff}}=\mu/\phi$ is the *effective viscosity* of the fluid in $\Omega_p$ and $\phi$ denotes the porosity of the porous media. In order to decide which model is adequate there exists a *rule of thumb*: the Brinkman model is used if the Reynolds numbers $\mathrm{Re}=\rho UL/\mu$ of the corresponding free flow is greater than 10. Here $U$ and $L$ are characteristic values for the velocity and the length of the whole problem.
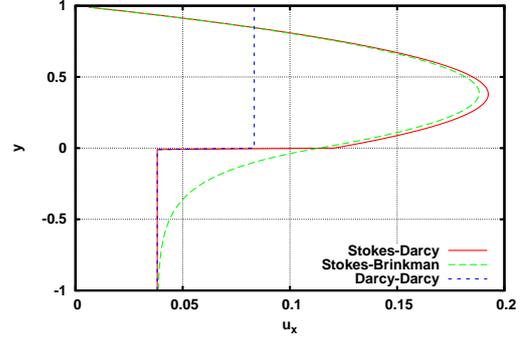


Fig. (**1**): Different ansatzes to model and to couple the problems in the free fluid flow region: Darcy, (Navier-)Stokes and in the porous flow region: Darcy, Brinkman, Brinkman-Darcy

## 3. INTERFACE CONDITIONS BETWEEN FLUID AND POROUS MEDIA (DARCY)

In this section we will discuss the aspects of proper interface conditions between different media. We consider in the sequel the (Navier–)Stokes equations (1) in the free fluid region $\Omega_f$, coupled across an interface with the Darcy equation (2) in the porous medium $\Omega_p$. This is the most common and mathematically the most difficult case, since these two models are completely different systems of partial differential equations. Hence, it is not clear what kind of conditions should be imposed at the interface $\Sigma$ between $\Omega_f$ and $\Omega_p$.

*Classical coupling conditions* for an inviscid fluid are the continuity of the pressure and the continuity of the normal velocities at the interface. For viscous flows, one would assume additionally the vanishing of the tangential velocity at the interface $\Sigma$.

Now, if the interface would be a boundary, then in the fluid part the system needs, e.g., a prescribed velocity ($N$ conditions) and the equation in $\Omega_p$ must be supplied with a given pressure or normal flux (1 condition). For coupling Darcy's model (2) and Stokes equation (1) some (well–known) interface conditions are needed to obtain a well–posed problem. Usually, these interface conditions describe the *continuity of the mass flux*

$$\mathbf{u}\cdot\mathbf{n}|_{\Sigma_p}=\mathbf{u}\cdot\mathbf{n}|_{\Sigma_f}, \qquad (4)$$

where $\Sigma_p$, $\Sigma_f$ is the same interface $\Sigma$ seen from porous and fluid parts. Let us note that eq. (4) is not sufficient to calculate the flow in $\Omega_p$, since the flux is yet unknown.

## 3.1 The Interface Conditions of Ene, Levy and Sanchez–Palencia

For the choice of further interface conditions we need a *classification of the flow*. This was done 1975 by Ene, Levy and Sanchez-Palencia [12, 31]: they distinguished two principally different cases of flow situations named in [25]:

**npf** (near parallel flow): the velocity in $\Omega_f$ is significantly larger than the filtration velocity in $\Omega_p$. The pressure gradients are of similar magnitude in both subdomains.

**nnf** (near normal flow): the velocities are of similar magnitude in both subdomains and the pressure gradient in $\Omega_f$ is significantly smaller than in $\Omega_p$ and nearly orthogonal to $\Sigma_p$.

Depending on this classification different interface conditions additional to (4) were proposed in [12, 31].

### 3.1.1 The Case of 'Near Parallel Flow'

For the case of *near parallel flow* Ene, Levy and Sanchez-Palencia [12, 31] suggested to use the conditions

$$\mathbf{u}|_{\Sigma_f} = 0, \qquad p|_{\Sigma_f} = p|_{\Sigma_p}. \tag{5}$$

The first condition in (5) originates from the *continuity of velocity* across the interface where the filtration velocity in $\Omega_p$ is neglected. Note that this simplification allows to compute (in principle) the flow solely in the domain $\Omega_f$. Hence, the pressure field is known in the fluid part $\Omega_f$ and via the *continuity of pressure* condition in (5) also on the interface $\Sigma_p$. Afterwards, the pressure field in the whole porous media can be determined by solving the elliptic Darcy equation (2) with prescribed pressure values on $\Sigma_p$. Doing so, one obtains a nonzero normal component of the filtration velocity in $\Omega_p$, i.e., the mass flux condition (4) holds only roughly.

### 3.1.2 The Case of 'Near Normal Flow'

For this case of *near normal flow* the authors proposed in [31] the interface conditions

$$\begin{aligned} p|_{\Sigma_p} &= C, \\ \mathbf{u} \cdot \tau_j|_{\Sigma_f} &= 0, \qquad j = 1, \ldots, N-1. \end{aligned} \tag{6}$$

$C$ denotes an a-priori unknown constant and $\tau_j$ are the orthogonal unit tangent vectors to the interface $\Sigma_f$. Since the pressure is usually defined only up to a constant, it is often convenient to assume that the pressure $p$ at the porous interface $\Sigma_p$ takes a certain (arbitrary) constant value $C$. Doing so, one neglects the dependence of $p|_{\Sigma_p}$ on the fluid flow in $\Omega_f$ (compared to the strong dependence in the porous media $\Omega_p$). For a chosen constant $C$ first the flow in $\Omega_p$ can be determined and then the problem in the fluid domain is solved using the mass flux condition (4) and the second condition in (6) for the tangential velocity components.

## 3.2 The Beavers–Joseph Interface Condition

In 1967 Beavers and Joseph [3] performed several experiments in a fluid channel over a porous media and found out that the mass flux through $\Omega_f$ is larger than predicted by the Poiseuille flow (i.e. with no-slip boundary conditions). This flow situation can be classified as a case of *near parallel flow* (cf. Section 3.1.1) with interface conditions (5). Beavers and Joseph explained this observation with a *slip velocity* at the interface and proposed an empirical *slip-flow condition* that agreed well with their experiments (cf. Fig. (**4**)):

$$\frac{\partial u}{\partial y}(x, 0+) = \frac{\alpha}{\sqrt{K}} \big( u(x, 0+) - u_D \big), \tag{7}$$

where $u_D$ denotes the uniform tangential (horizontal) Darcy velocity in $\Omega_p$ ($-H < y < 0$) obtained from the Darcy equation (2) and $u(x, 0+)$ is the tangential velocity component in the fluid region $\Omega_f$ ($0 < y < G$) and $K$ denotes the permeability. This interface condition (7) relates the gradient of the free flow velocity at the interface $y = 0$ to the filtration velocity $u_D$. The Beavers–Joseph constant $\alpha$ (measured slip coefficient) in eq. (7) only depends on porous media properties. It denotes a dimensionless quantity depending on the material parameters which characterize the structure of the permeable material within the boundary region and its values ranges between 0.01 and 5 [34]. Let us point out that eq. (7) allows for a discontinuity in the tangential velocity, i.e., rapid changes in the velocity in a small boundary layer are substituted through a jump. Using the Beavers–Joseph condition (7) the agreement between measurements from their experiments and the predicted values was quite good, with over 90% of the experimental values having errors of less than 2% [3]. The work of Beavers and Joseph was continued by investigations of Taylor [46] and Richardson [40] and an extension, the *Jones condition*, was proposed in [24].
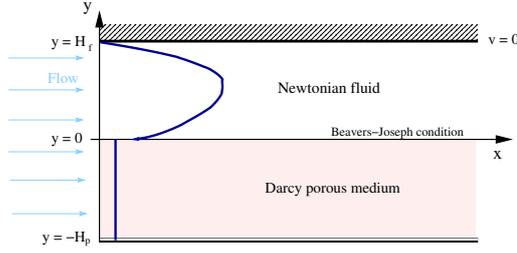
Fig. (**2**): Two–layer configuration for Poiseuille flow overlying a porous medium (Darcy): velocity is significantly discontinuous at interface

Later on Payne and Straughan [38] showed the continuous dependence of the solution on the Beavers–Joseph constant $\alpha$ in eq. (7). Moreover, the interface condition eq. (7) was mathematically justified by Jäger and Mikelić [20, 21]. Although this condition is not justified in the general case, it is widely used in practical computations for coupled fluid flows, e.g., in [8, 28, 32, 41, 47] and especially many tests in [6].

We note that in the original paper by Beavers and Joseph [3], the coupling condition (7) has been derived in order to interpret an experiment with parallel channel flow in a porous medium and free space, very much similar to the structure proposed here. In their experiment, the amounts of fluid leaving the device at the porous part and at the free flow part have been separated, and measured for different values of the pressure drop. For this setting the exact analytical solution is easily obtained [6], and can be used in transport computations.

## 3.3 Saffman's Modification of the Beavers–Joseph Interface Condition

In the article [42] Saffman gave a 'theoretical' justification of the Beavers–Joseph interface condition at a physical level of rigor. Moreover, Saffman proposed in 1971 a modification of the Beavers–Joseph law (7): he found out that the tangential velocity on the interface is proportional to the shear stress and proposed a modification of the Beavers–Joseph condition:

$$u(x,0+) = \frac{\sqrt{K}}{\alpha}\frac{\partial u}{\partial y}(x,0+) + O(K). \quad (8)$$

While the Beavers–Joseph interface condition (7) couples the fluid velocity in $\Omega_f$ with the filtration velocity in $\Omega_p$, the modified eq. (8) (Beavers–Joseph–Saffmann condition) contains only variables

in the free fluid domain $\Omega_f$ where the filtration velocity is usually much smaller than the slip velocity $u(0)$. If the slip velocity is smaller than the maximal filtration velocity then setting the tangential velocity to zero is a reasonable approximation. We remark that Dagan [7] came in 1979 to the same conclusion. He proposed a so-called Slattery's relation [44] between the pressure gradient and the first two derivatives of the Darcy velocity in order to obtain the condition (8).

## 4. INTERFACE CONDITIONS BETWEEN FLUID AND POROUS MEDIA (BRINKMAN)

Neale and Nader [36] suggested in 1974 the usage of the Brinkman correction to the Darcy model (3): they proposed to assume continuity of velocity and stress (using $\mu_{\text{eff}}$) across the fluid–porous interface since the Stokes and the Brinkman equation are of the same order. Doing so, Neal and Nader obtained in the fluid region the same solution as Beavers and Joseph provided that the slip coefficient is chosen as $\alpha = \sqrt{\mu_{\text{eff}}/\mu}$. An exact analytical solution for a velocity profile in $x$ direction can be found in [16].

Vafai and Kim [48] constructed 1990 an exact analytic solution for the interface region, including boundary and inertia effects. Later on, Alazmi and Vafai [1] classified and analyzed five primary categories of interface conditions between fluid layer and porous medium (modelled by Brinkman eq. (3)).

In 1992 Sahraoui and Kaviany [43] performed a numerical study and calculated the slip coefficient: they discovered that the Brinkman extension to the Darcy equation does not satisfactorily model the flow field in $\Omega_p$ . However, this can be overcome using a variable effective viscosity $\mu_{\text{eff}}$ in the porous medium.

On the contrary, for the Brinkman model for the flow in $\Omega_p$ this ambiguity does not occur. In this case, the equations in the porous media $\Omega_p$ and equations in the fluid region $\Omega_f$ are of the same type. Two types of coupling conditions can be found in the literature. The more common choice are conditions of *continuous velocity* and *continuity of the normal component of the stress tensor*

$$\mathbf{u}|_{\Sigma_p} = \mathbf{u}|_{\Sigma_f} \quad (9)$$

$$\mathbf{n}\cdot(\mu_{\text{eff}}\nabla\mathbf{u}-p\mathbf{I})|_{\Sigma_p} = \mathbf{n}\cdot(\mu\nabla\mathbf{u}-p\mathbf{I})|_{\Sigma_f}, \quad (10)$$

where $\Sigma_p$, $\Sigma_f$ is the same interface $\Sigma$ seen from porous and fluid parts. Such conditions would naturally arise, if for some reasons (e.g. in the domain

decomposition approach), the fluid region is divided into subdomains, where the Navier–Stokes equations are valid. Usually, the condition (9) is the first one out of $N$ conditions on the interface when considering a Stokes–Brinkman system. This approach is used numerically in [19, 27].

## 4.1 The Stress Jump Conditions of Ochoa-Tapia and Whitaker

Ochoa-Tapia and Whitaker [37] obtained 1995 at the interface continuity of the velocity and the continuity of the 'modified' normal stress by a volume averaging technique of the momentum equations in the interface region. In their analysis they showed that the matching of Stokes equation with the Brinkman model conserves the continuity of velocity but induces a jump in the shear stress. Hence, they proposed additionally to the condition (9), a *stress jump condition* that takes into account the momentum transfer at the interface

$$\frac{\partial u}{\partial y}(x, 0+) - \frac{1}{\phi_p}\frac{\partial u}{\partial y}(x, 0-) = -\frac{\beta}{\sqrt{K}}u. \quad (11)$$

Here, $\beta$ denotes a dimensionless parameter of order one that is defined as a solution of a closure problem. The authors investigated in [37] the conditions (9), (11) in a 1D channel geometry and compared the results with the classical Beavers–Joseph experiment. These boundary conditions proposed in [37] were used by Kuznetsov [26] to compute solutions in channels partially filled with a porous material.

Many attempts have been made to estimate the adjustable jump coefficient $\beta$ or to obtain an expression for $\beta$, depending on the microstructure of the interface region. In [49] the authors derived a stress jump boundary condition at the interface *free of adjustable coefficients*. The associated local closure problems, modelling the microstructure of the interface, determine a mixed stress tensor which is the reason for the jump.

Furthermore, only few authors have studied the physical nature of these jump coefficients. Jamet and Chandesris [22, 23] analyzed the physical meaning based on an upscaling method of the transport equations in the interfacial region. Doing so, they were able to interpret the jump coefficients as surface tension quantities depending linearly on the position of the interface.

In the dissertation of Laptev [27] a new numerical method in 3D using these interface conditions (9), (11) was proposed. Furthermore, the mathematical model of the coupling of Navier–Stokes and
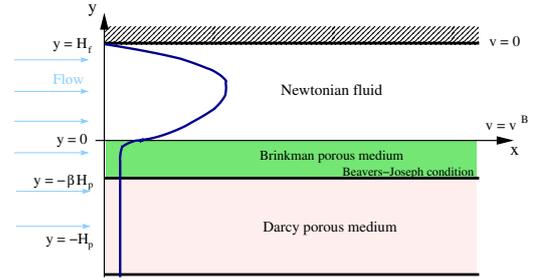


Fig. (**3**): Three–layer configuration for Poiseuille flow overlying a porous medium with Brinkman transition layer: still discontinuity in velocity between Brinkman and Darcy layers with relative error $\gamma \sim 1/\beta$ of lower order

Brinkman equations using the stress tensor jump interface condition (11) was validated for a large class of model problems [27].

## 4.2 The Transition Zone Approach

There are serious doubts about the validity of the Brinkman equation, e.g. for the case of lower porosities [33, 17], whereas Darcy's law is not disputed for this case. The Brinkman model suffers from at least three limitations: first it is only valid for materials with high porosity, secondly, the effective viscosity $\mu_{\text{eff}}$ used in this model may change discontinuously at the interface. Finally, as a rule of thumb, the Brinkman model should only be used if the Reynolds numbers $\text{Re} = \rho UL/\mu$ of the corresponding free flow is greater than 10. Here $U$ and $L$ are characteristic values for the velocity and the length of the whole problem.

On the other hand, it appears to be useful to introduce a transition layer between Stokes and Darcy flow, which may be described by the Brinkman equation.

When studying a Poiseuille flow over a permeable region, e.g., by Chandesris and Jamet [5], in turned out that the sharp interface with its jump conditions is only the limiting case (i.e. an idealization) of a *transition region*, where the physical properties of the medium have a strong but still continuous variations. Actually, this idea goes back to Nield [33]. He proposed 1983 to use a Brinkman equation in the transition region between the fluid and the porous medium modeled by the Darcy equation. This approach was also validated experimentally by Goharzadeh et al. [15]. They found out experimentally that the thickness of the transition region should be of the same order as the grain size of the porous

medium.

In 2003, Goyeau et al. [16] studied the momentum balance at the interface of a two-layer system and introduced a heterogeneous continuously varying transition zone between the 'outer' fluid and porous zones. The authors derived an explicit formula for the stress jump coefficient $\beta$ involved in the momentum transport. However, this approach assumes the knowledge of the spatial dependence of the effective quantities in the region around the interface.

Chandesris and Jamet [5] solved in 2006 the problem in this transition zone using the technique of *matched asymptotic expansions*: they obtained an explicit representation of the stress jump coefficient in the transition zone depending only on the parameters of the porous medium (permeability and porosity).

Recently, Hill and Straughan [17] considered a *three-layer* constellation: a free fluid interfacing a Brinkman-type porous transition layer, which overlies a porous medium modelled by the Darcy eq. (2). The authors gave the exact analytical solution for the velocity profile and discovered two instability modes that depend on the ratio of the thickness parameters of the different layers. Also, Nield and Kuznetsov [35] derived exact solutions using Airy functions for a transition layer considering a shear flow in a channel.

## 4.3 The Interface Conditions of Le Bars and Worster

Recently, Le Bars and Worster [29] considered special 'analytically tractable' cases for the one-domain approach with the Brinkman model for the porous medium. The authors compared their findings with the two-domain approach of Section 4 using the Darcy equation and its previously proposed interface conditions, especially the Beavers–Joseph condition (7). Le Bars and Worster considered the Brinkman equation in the configuration studied by Beavers and Joseph, and found a new condition at the fluid-porous interface

$$u(x, -\delta+) = u_D(x, -\delta), \qquad \text{with } \delta = c\sqrt{K}, \tag{12}$$

where $c$ is a constant of order 1. They defined a *viscous transition zone* inside $\Omega_p$, where the Stokes equation still applies up to a depth $\delta$, and imposed continuity of pressure and velocities (9) at the position $y = -\delta$ (cf. Fig. (**4**)). Here, $\delta$ denotes the characteristic size of this transition zone (a few pore

lengths). Using this new condition (12) the computed values have a (slightly) better coincidence with the experimental values of Beavers and Joseph. Let us remark that the authors of [16, 29] found good agreement between the single-domain approach of Section 4 and the two-domain approach of Section 3. However, this can be explained by the special configurations, cf. [18], namely a one-dimensional tangential flow in [16] and a seemingly very small vertical velocity gradient on the interface in [29].
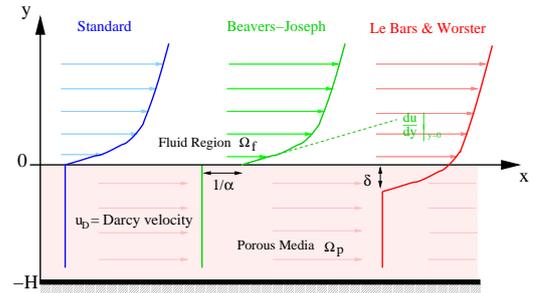


Fig. (**4**): Comparison of Different Interface Models for Porous Media: From left to right: The standard case: no-slip condition on the fluid–porous interface, the Beavers–Joseph condition (7): slip of size $1/\alpha$ on the fluid–porous interface and the Le Bars and Worster condition (12): slip by $\delta$ into the porous media.

# 5. APPLICATION TO A FLOW CELL

The spatial domain $\Omega$ under consideration with co-ordinate functions $(x,y)$ is described as: $\bar{\Omega} = \bar{\Omega}_p \cup \bar{\Omega}_f$, where $\Omega_f = (0,L) \times (0,H_f)$ is the free flow domain, and $\Omega_p = (0,L) \times (-H_p,0)$ denotes the porous part, cf. Fig. (**5**).

We characterize the porous medium with respect to the fluid flow by its permeability $K = K(\varepsilon)$, and with respect to species transport by its dispersion coefficient $D_p$. In order to simplify the discussion we relate both to the porosity $\varepsilon$ of the porous medium. More precisely, we use the *Karman-Kozeny equation* [2]

$$K = K_0 \frac{\varepsilon^3}{(1-\varepsilon)^2} \tag{13}$$

and the *Bruggeman correlation* $D_p = D_f \varepsilon^{\frac{3}{2}}$, cf. [39].

We consider a steady-state flow process in a free flow domain modeled by the *incompressible Navier-Stokes equation* (1)
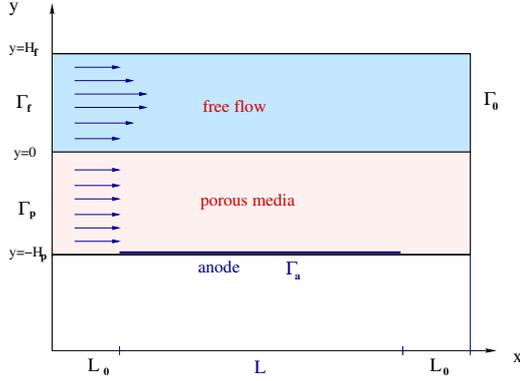
Fig. (**5**): Schematic of a flow cell with porous diffusion layer

.

Every channel flow profile satisfies the *no-slip condition* at the impermeable wall

$$\mathbf{u}(y) = 0 \quad \text{at } y = H_f, \qquad (14)$$

and due to the incompressibility condition $\nabla \cdot \mathbf{u} = 0$ one immediately obtains the continuity of the normal velocity across the fluid-porous interface at $y = 0$.

We assume several flow profiles in the joint domain which are motivated by different approaches to model and to couple the problems in the free and porous flow regions. For all flow profiles, let $1/\mu \nabla p = (\delta_p, 0)^\top$ be the constant pressure gradient with $\delta_p < 0$.

## 5.1  Species transport modeling

At fixed temperature $T$ and fixed pressure $p$, a $H_2SO_4$ based electrolyte containing dissolved $H_2$ enters the cell at the inlet, flows over the anode, and leaves the cell at an outlet. At the inlet, the solute concentration is given by a value $c_I$, which depends on the pressure and the temperature. $H_2$ is transported to the anode and reacts at the catalytic surface according to

$$H_2 \rightarrow 2H^+ + 2e^-, \qquad (15)$$
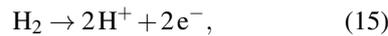
creating two electrons and two protons per reacted molecule. The amount of electrons generated during this reaction is measured as an electrical current. For high enough ion concentration due to the support electrolyte, ohmic potential drops are negligible. Furthermore, the reaction rate of hydrogen oxidation is large in comparison to the transport processes in the cell, therefore we say that it is *purely*

*transport limited*. The current $I$ measured in such a situation is called *limiting current*.

## 5.2  Transport equation

According to [13, 14] the stationary species transport (convection and diffusion) in such a flow cell can be described by the partial differential equation

$$\nabla \cdot (D(x,y)\nabla c - c\mathbf{u}(x,y)) = 0 \quad \text{in } \Omega \qquad (16)$$

supplied with the incompressibility condition $\nabla \cdot \mathbf{u} = 0$. Here, $D$ is the molecular diffusion coefficient and $c = c(x,y)$ denotes the concentration of a dissolved species.

Let us assume that the diffusion coefficient $D = D(x,y)$ is piecewise constant: $D(x,y) = D_f$ for $y > 0$ and $D(x,y) = D_p$ for $y < 0$ and for the velocity profile, we assume $\mathbf{u}(x,y) = (u_x(y), 0)^\top$ with a given $x$ component $u_x(y)$. In the sequel, we will write shortly $u(y)$ instead of $u_x(y)$. We consider the following boundary conditions:

**free flow inlet:** $c = c_f$ on $\Gamma_f = 0 \times (0, H_f)$

**porous inlet:** $c = c_p$ on $\Gamma_p = 0 \times (-H_p, 0)$

**anode:** $c = 0$ on $\Gamma_a = (L_o, L - L_o) \times -H_p$

**outlet:** $\frac{\partial c}{\partial \mathbf{n}} = 0$ on $\Gamma_o = L \times (-H_p, H_f)$

On all other parts of the domain, we assume *no flow boundary conditions*

$$(D(x,y)\nabla c - c\mathbf{u}(x,y)) \cdot \mathbf{n} = 0. \qquad (17)$$

The values $c_f$, $c_p$ in the boundary conditions denote the inlet concentrations. The boundary concentration at the anode will be assumed to be 0, modeling a surface reaction with infinitely fast kinetics. For reaction (15), the limiting current can be calculated from the amount of solute leaving the domain at the anode as

$$I = 2F \int_{\Gamma_a} (D(x,y)\nabla c - c\mathbf{u}(x,y)) \cdot \mathbf{n} \, ds. \qquad (18)$$

## 5.3  Asymptotic models

Due to the lack of analytical solutions, asymptotic models based on boundary layer theory have been used for a long time to derive quantitative estimates. For the channel flow with an infinite strip electrode, the solution was given in [30]. In [13] the following expression for the limiting current was established

$$I = 2FD(c_I - c_0)\frac{A}{L}\text{Sh}, \qquad (19)$$

where $F$ the Faraday constant and

$$\text{Sh} = \frac{3^{\frac{4}{3}}}{2\Gamma(\frac{1}{3})}\,\text{Pe}^{\frac{1}{3}} \approx 0.8075491\,\text{Pe}^{\frac{1}{3}}, \qquad (20)$$

is the dimensionless Sherwood number, $D$ the diffusion coefficient and $A$ is the electrode surface, which in this case is equal to $L$. The dimensionless Peclet number Pe is defined by $\text{Pe} = 6\bar{v}L^2/(DH_f)$.

## ACKNOWLEDGEMENT

## REFERENCES

[1] Alazmi B, Vafai K. Analysis of fluid flow and heat transfer interfacial conditions between a porous medium and a fluid layer. Int J Heat Mass Transfer 2001; 44: 1735-1749.

[2] Arampatzis G, Assimacopoulos D. Numerical modeling of convection-diffusion phase change problems. Comput Mech 1998; 21: 409-415.

[3] Beavers G, Joseph DD. Boundary conditions at a naturally permeable wall. J Fluid Mech 1967; 30: 197-207.

[4] Brinkman HC. A calculation of the viscous force exerted by a flowing fluid on a dense swarm of particles. Appl Sci Res 1948; A1: 27-34.

[5] Chandesris M, Jamet D. Boundary conditions at a planar fluid-porous interface for a Poiseuille flow. Int J Heat Mass Transfer 2006; 49: 2137-2150.

[6] Chang MH, Chen F, Straughan B. Instability of Poiseuille flow in a fluid overlying a porous layer. J Fluid Mech 2006; 564: 287-303.

[7] Dagan G. Generalization of Darcy Law for Nonuniform Flows. Water Res Res 1979; 15: 1-7.

[8] Discacciati M, Miglio E, Quarteroni A. Mathematical and numerical models for coupling surface and groundwater flows. Appl Num Math 2002; 43: 57-74.

[9] Discacciati M. Domain decomposition methods for the coupling of surface and groundwater flows. PhD thesis, École Polytechnique Fédérale de Lausanne, 2004.

[10] Ehrhardt M, Fuhrmann J, Holzbecher E, Linke A. Mathematical Modeling of Channel-Porous Layer Interfaces in PEM Fuel Cells. in: B. Davat B, Hissel D (eds.). Proceedings of 'FDFC2008 - Fundamentals and Developments of Fuel Cell Conference 2008'. Nancy, France.

[11] Ehrhardt M, Fuhrmann J, Linke A. A model of an electrochemical flow cell with porous layer. Preprint No 09/04, October 2009, (submitted to: Networks and Heterogeneous Media).

[12] Ene HI, Sanchez-Palencia E. Equations et phénomènes de surface pour l'écoulement dans un modèle de milieu poreux. J Mécan 1975; 14: 73-108.

[13] Fuhrmann J, Zhao H, Holzbecher E, Langmach H, Chojak M, Halseid R, Jusys Z, Behm, R. Experimental and numerical model study of the limiting current in a channel flow cell with a circular electrode. Phys Chem Chem Phys 2008; 10: 3784-3795.

[14] Fuhrmann J, Zhao H, Holzbecher E, Langmach H. Flow, transport, and reactions in a thin layer flow cell. J Fuel Cell Sci Techn 2008; 5: 021008/1-021008/10.

[15] Goharzadeh A, Khalili A, Jorgensen BB. Transition layer thickness at a fluid-porous interface. Phys Fluids 2005; 17: 057102/1-057102/10.

[16] Goyeau B, Lhuillier D, Gobin D, Velarde MG. Momentum transport at a fluid-porous interface. Int J Heat Mass Transfer 2003; 46: 4071-4081.

[17] Hill AA, Straughan B. Poiseuille flow in a fluid overlying a porous medium. J Fluid Mech 2008; 603: 137-149.

[18] Hirata SC, Goyeau B, Gobin D, Carr M, Cotta RM. Linear stability of natural convection in superposed fluid and porous layes: Influence of the interfacial modelling. Int J Heat Mass Transfer 2007; 50: 1356-1367.

[19] Iliev O, Laptev V. On numerical simulation of flow through oil filters. Comput Visual Sci 2004; 6: 139-146.

[20] Jäger W, Mikelić A. On the boundary conditions at the contact interface between a porous medium and a free fluid. Ann Sc Norm Super Pisa, Cl Sci IV 1996; 23: 403-465.

[21] Jäger W, Mikelić A. On the interface boundary condition of Beavers, Joseph, and Saffman. SIAM J Appl Math 2000; 60: 1111-1127.

[22] Jamet D, Chandesris M. Boundary conditions at a fluid-porous interface: an a priori estimation of the stress jump coefficients. Int J Heat Mass Transfer 2007; 50: 3422-3436.

[23] Jamet D, Chandesris M. On the intrinsic nature of jump coefficients at the interface between a porous medium and a free fluid region. Int. J. Heat Mass Transfer 2009; 52: 289-300.

[24] Jones IP. Low Reynolds number flow past a porous spherical shell. Proc Camb Philos Soc 1973; 73: 231-238.

[25] Kaviany M. Principles of Heat Transfer in Porous Media. Springer, New York, 1991.

[26] Kuznetsov AV. Influence of the stress jump boundary condition at the porous-medium/clear-fluid interface on a flow at a porous wall. Int Commun Heat Mass Transfer 1997; 24: 401-410.

[27] Laptev V. Numerical solution of coupled flow in plain and porous media, PhD thesis, Universität Kaiserslautern, Germany, 2003.

[28] Layton WJ, Schieweck F, Yotov I. Coupling Fluid Flow with Porous Media Flow. SIAM J Numer Anal 2003; 40: 2195-2218.

[29] Le Bars M, Worster MG. Interfacial conditions between a pure fluid and a porous medium: implications for binary alloy solidification. J Fluid Mech 2006; 550: 149-173.

[30] Lévêque A. Annales des Mines 1928; 13: 201-299, 305-362, 381-415.

[31] Levy T, Sanchez-Palencia E. On boundary conditions for fluid flow in porous media. Int J Eng Sci 1975; 13: 923-940.

[32] Miglio E, Quarteroni A, Saleri F. Coupling of free surface and groundwater flows. Comput. Fluids 2003; 32: 73-83.

[33] Nield DA. The boundary correction for the Rayleigh-Darcy problem: limitations of the Brinkman equation. J Fluid Mech 1983; 128: 37-46.

[34] Nield DA, Bejan A. Convection in Porous Media. 3rd edition, Springer, New York, 2006.

[35] Nield DA, Kuznetsov AV. The effect of a transition layer between a fluid and a porous medium: shear flow in a channel. Transp Porous Med 2009; 78: 477-487.

[36] Neale G, Nader W. Practical significance of Brinkman extension of Darcy's law: coupled parallel flows within a channel and a bounding porous medium. Can J Chem Eng 1974; 52: 475-478.

[37] Ochoa-Tapia JA, Whitaker S. Momentum transfer at the boundary between a porous medium and a homogeneous fluid. I. Theoretical development., II. Comparison with experiment. Int J Heat Mass Transfer 1995; 38: 2635-2656.

[38] Payne LE, Straughan B. Analysis of the boundary condition at the interface between a viscous fluid and a porous medium and related modelling questions. J Math Pures Appl 1998; 77: 317-354.

[39] Pharoah JG, Karan K, Sun W. On effective transport coefficients in PEM fuel cell electrodes: Anisotropy of the porous transport layers. J Power Sources 2006; 161: 214-224.

[40] Richardson SA. A model for the boundary conditions of a porous material, Part 2. J Fluid Mech 1971; 49: 327-336.

[41] Rivière B. Analysis of a discontinuous finite element method for the coupled Stokes and Darcy problems. J Sci Comput 2005; 22: 479-500.

[42] Saffman PG. On the boundary condition at the interface of a porous medium. Stud Appl Math 1971; 1: 93-101.

[43] Sahraoui M, Kaviany M. Slip and No-Slip Velocity Boundary Conditions at Interface of Porous, Plain Media. Int J Heat Mass Transfer 1992; 35: 927-944.

[44] Slattery JC, Sagis L, Eun-Suok Oh. Interfacial Transport Phenomena. Springer, 2nd edition, 2007.

[45] Straughan B. Stability and Wave Motion in Porous Media. Applied Mathematical Sciences 165, Springer, 2008.

[46] Taylor GI. A model for the boundary conditions of a porous material, Part 1. J Fluid Mech 1971; 49: 319-326.

[47] Urquiza, JM, N'Dri D, Garon A, Delfour MC. Coupling Stokes and Darcy equations. Appl Numer Math 2008; 58: 525-538.

[48] Vafai K, Kim SJ., 1990, Fluid mechanics of the interface region between a porous medium and a fluid layer – an exact solution. Int J Heat Fluid Flow 1990; 11: 254-256.

[49] Valdés-Parada FJ, Goyeau B, Ochoa-Tapia JA. Momentum Stress Jump Condition at the Fluid-Porous Boundary: Prediction of the Jump Coefficient. Proceedings of the AIChE National Meeting, San Francisco, USA, November 12-17, 2006.